J. Phys.: Condens. Matter 5 (1993) 7049–7062. Printed in the UK

Defect electronic states in β-carotene and lower homologues

R M Valladares†, W Hayes†, A J Fisher† and A M Stoneham‡

† Clarendon Laboratory, Parks Road, Oxford OX1 3PU, UK

‡ AEA Industrial Technology, Harwell Laboratory, Didcot, Oxon OX11 0RA, UK

Received 14 June 1993

Abstract. We present semi-empirical calculations of the atomic geometries and electronic charge distributions of β-carotene homologues of different chain lengths. We find defects in charged and photoexcited chains that are similar to the defects found in the degenerate polymer *trans*-polyacetylene, and we show how confinement affects these defects as the chains are shortened. Our results exhibit a generalized form of charge-conjugation symmetry in which the properties of a negatively charged defect are related to those of a positive one and *vice versa*.

1. Introduction

Conjugated polymers have attracted much attention as candidate device materials since the discovery that they could be reversibly doped by electrochemical methods (Chiang *et al* 1977), and the proposal (Su *et al* 1979, 1980) that the strong electron–phonon coupling should produce novel coupled excitations of the electron–lattice system. This proposal yielded a great deal of interesting physics, indicating the existence of a range of defects such as solitons, excitons, polarons, bipolarons and breathers. A review of the extensive literature in this field is given by Heeger *et al* (1988).

The Su–Schrieffer–Heeger (henceforth SSH) model focuses on the coupling between the π electrons, described by a simple tight-binding model, and the bond lengths along the carbon backbone of the polymer. In the SSH description, the polymer is driven from a one-dimensional metallic state to a semiconducting one by a Peierls transition, resulting in a bond-length alternation along the backbone of the polymer characterized by a non-zero value of the dimerization parameter d_n, which is defined by

$$d_n = (-1)^n(b_{n-1,n} - b_{n,n+1}) \tag{1}$$

where $b_{n,n+1}$ is the bond length between the nth and $(n+1)$th atoms of the carbon backbone. This naturally leads to a division of conducting polymers into two classes: first the *degenerate polymers*, in which there are two degenerate ground states with equal uniform dimerizations of opposite sign (i.e., a symmetry is spontaneously broken by the Peierls transition), and second the *non-degenerate polymers*, which have an intrinsic preference for one sign of dimerization over the other. The defects found in the two classes differ in that a degenerate polymer can tolerate an arbitrarily long length of chain with reversed dimerization, so pairs of soliton (or bond-alternation) defects feel no mutual interaction at large distances. In a non-degenerate polymer, however, such a region of reversed dimerization costs energy and soliton pairs feel a confining force as a result.

0953-8984/93/387049+14$07.50

The SSH model in its simplest form has a number of special features. One is the charge-conjugation symmetry (CCS) that it exhibits, which results from the invariance of the Hamiltonian

$$H = -\sum_n \sum_s [t_0 - \alpha(u_{n+1} - u_n)]\left(c_{ns}^+ c_{n+1,s} + c_{n+1,s}^+ c_{ns}\right) + \frac{1}{2}K \sum_n (u_{n+1} - u_n)^2 \qquad (2)$$

under the transformation $c_{ns}^+ \rightarrow (-1)^n c_{ns}$ (where c_{ns}^+ and c_{ns} represent the creation and annihilation operators for p_z electrons of spin s at site n and u_n is the displacement of the nth atom from its undimerized position). The Hamiltonian possesses this symmetry as a consequence of the restriction to nearest-neighbour hopping matrix elements and the lack of any explicit electron–electron interaction terms. The symmetry causes the one-electron energy spectrum to be exactly symmetric about mid-gap, and imposes additional selection rules on interlevel transitions. In addition, the absence of interaction between the electrons gives artificial results, such as an overestimate of the stability of bipolaronic defects in degenerate polymers; in reality, the mutual repulsion of two charges causes them to decay into pairs of charged solitons. These special features are one reason for wishing to go beyond this simple model. Another is that the very generality of the model precludes its use to study the properties specific to different types of polymer. This is a subject of great current interest.

The simplest polymers displaying degenerate and non-degenerate properties are *trans*- and *cis*-polyacetylene respectively (see Roth and Bleier (1987) and references therein); an enormous amount has been learned from systematic studies of the optical and transport properties of both these isomers as a function of doping. However there has been much recent activity in two related areas: the first is the study of shorter chains, while the second is the study of different polymers with more complicated structures. The systematic study of short chains of well defined length illuminates the connection between the properties of polymers and of oligomers (Brédas *et al* 1983, Brédas and Heeger 1989, Brédas and Toussaint 1990, Kohler 1991, Shuai and Brédas 1992), while polymers other than polyacetylene have special advantages in materials processing and for particular applications such as light-emitting diodes (Burroughes *et al* 1990).

In this paper, we describe calculations on oligomers of the β-carotene family. β-carotene is of intrinsic interest because it is implicated in the photosynthetic process and acts as a precursor for other biologically important molecules such as retinene and vitamin A. Its optical properties have been studied for a number of years—see, for example, Rosenberg (1959). However, the material may also be viewed as a finite degenerate polymer, similar in many respects to *trans*-polyacetylene but having methyl side groups at intervals along the chain instead of simple hydrogen atoms, and terminated at each end by a ring (see figure 1). One double bond on the ring terminates the π-electron system of the chain, the rest of the ring being composed of saturated sp^3-bonded carbon atoms. The similarity of β-carotene to *trans*-polyacetylene makes it a natural candidate for investigation as a conducting material; it has now been shown that it can be doped p type by exposure to either iodine or AsF_5 (Ehrenfreund *et al* 1992a, b). Optical evidence suggests that charged defects are formed similar to those found in polyacetylene (Ehrenfreund and Coter 1991), and that charge storage on the chains is in the form of a spinless species; calculations suggest that this species comprises a pair of charged solitons at opposite ends of the chain part of the molecule (Ehrenfreund *et al* 1992a, b).

Recently, Andersson *et al* (1992) were able to synthesize and study separately a homologous series of molecules with three, five, seven, nine and eleven double bonds

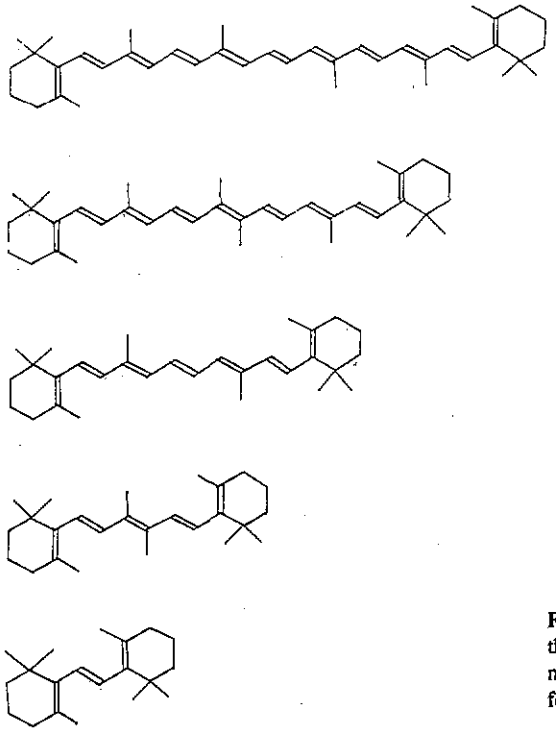

Figure 1. Molecular structures of β-carotene and the lower homologues studied in this paper. The methyl side chains are replaced by hydrogen atoms for the purposes of our calculations.

(see figure 1). We shall follow their nomenclature and refer to the molecules as mini-3 through to mini-11 (β-carotene itself). We have examined theoretically the same range of oligomers in the β-carotene family, using a semi-empirical self-consistent molecular orbital program (Wallace *et al* 1991a, b) to calculate the minimum-energy atomic geometries for different charge and spin states of the molecule. Our method takes full account of the atomic geometry of the molecule, and includes both a self-consistent treatment of electron–electron interactions and long-range hopping terms that break the simple CCS symmetry of the SSH model. We have examined the dimerization (calculated along the chain part of the molecule and on the π-bonded portion of the end rings) and charge distributions as a function of the chain length.

In the remainder of the paper we first present a brief description of our computational technique, followed by the results of our calculations on neutral chains in their singlet ground state, doubly charged chains, singly charged chains and finally neutral chains in which one electron is excited to a triplet state to form an exciton. We conclude with a discussion of the confinement effects induced by the presence of the chains, and of the modified CCS that we find to hold in these systems.

2. Methodology

Owing to the strong electron–lattice coupling in conjugated polymers it is necessary to perform self-consistent calculations of electronic wave functions and atomic positions in order to be able to study the defects responsible for their behaviour. The method (Wallace *et al* 1991a) used here to perform these calculations enables semi-empirical Hartree–Fock (HF) theory to be used in this self-consistent way by solving the HF equations simultaneously

with the classical Newtonian dynamical equations of motion for the ions. The numerical calculations have been carried out with the CNDO (complete neglect of differential overlap) parametrization of HF theory. While we do not believe that such a semi-empirical approach represents the last word in accuracy, we have found it to give reliable geometries in our previous work on conjugated materials (Wallace *et al* 1991a, b, Fisher *et al* 1991). We prefer to use this parametrization consistently for all the properties we calculate (geometries, charge distributions and energies) rather than use different schemes for different properties.

The first successful method to treat the optimization of self-consistent electronic structure and geometry as a single problem was that due to Car and Parrinello (1985), who used density-functional theory in the local-density approximation and a plane-wave basis set to represent the electronic structure. The Car–Parrinello method involves assigning fictitious masses to the electron wave functions and treating them as classical dynamical variables as one would the atomic positions. Using the Euler–Lagrange equations of motion the resulting system is then allowed to evolve in time. Instead, our wave-function calculation involves the recursive diagonalization of an $N \times N$ matrix (N being the number of basis orbitals used), which is the time-limiting step of the calculation. Since this calculation is carried out in parallel with the molecular geometry calculation just a few steps (typically one) of the recursion are performed at each molecular geometry encountered along the minimization path. Both our technique and the original Car–Parrinello approach use a molecular-dynamics method with simulated annealing for the atomic motion to find the minimum-energy configuration. Since this relaxation in our method is done using a dynamical technique, it does not require second derivatives to be calculated. The first derivatives are calculated analytically using the Hellman–Feynman theorem. While not having the accuracy of *ab initio* electronic-structure methods, this approach has the advantage of employing a calculation of the electronic structure that is well tested for organic materials and that allows typical polymer chains to be treated entirely self-consistently with very modest computational resources.

The strengths of our method lie in its ability to represent the geometries of organic molecules in a very wide variety of chemical environments. The essential features of charge self-consistency and response of atoms to their bonding environment are captured. On the other hand, the limited flexibility of the basis set inevitably restricts the ability of the electrons to respond to distortions of the molecule; this, combined with the intrinsic limitations of the HF technique, causes vibrational frequencies to be overestimated by factors of about 1.4 (Wallace *et al* 1991a, b). It also shares with other methods (including *ab initio* approaches) difficulties in predicting the properties of excited states. We have found that one-electron energy differences substantially overestimate excitation energies, although taking differences of total energies, where this is possible, is much more reliable; we give examples of such calculations in sections 3.1 and 3.4.

3. Results and discussion

The method outlined in section 2 is applied here to the study of defects in the molecule *trans*-β-carotene (11 conjugated double bonds) and its series of lower homologues mini-3, mini-5, mini-7 and mini-9 with three, five, seven and nine conjugated double bonds respectively (see figure 1). The backbone of β-carotene consists of alternating single and double bonds which differ in length. The distortion can be characterized by the so-called dimerization parameter (equation (1)). Although β-carotene is not strictly a conjugated polymer, the length of the central section (polymer backbone) is such that one would expect this molecule to display

similar behaviour to and have properties characteristic of other conducting polymers such as *trans*-polyacetylene (*t*-PA). If we neglect the influence of the chain ends, the *t*-PA and β-carotene systems both possess a degenerate ground state; this means that each can be described by a double-well potential where the two wells (corresponding to different senses of bond alternation) have exactly the same energy. In short chains such as those we consider in this paper, however, this degeneracy is lifted and a preferred sense of bond alternation is enforced by the terminating groups. The methyl groups along the molecule (see figure 1) were replaced by hydrogen atoms in the calculations. This is a valid approximation when studying these molecules, given that the states that determine their behaviour in the presence of the defects are those with electrons in π orbitals (sp^2 hybridization) located along their backbones, whereas the methyl groups have sp^3 bonding which means that all the valence electrons are localized in strongly directed σ-type orbitals.

Our calculations were started from a configuration in which the polymeric backbone of each molecule was planar. We found no significant deviations from planarity during the calculations along the backbone of the molecules and in the carbon atoms of the terminating rings; however, the hydrogen atoms in the unsaturated parts of the rings (figure 1) do not lie in the same plane as the backbone. As discussed in section 2 the ground state was reached using damped molecular dynamics. The valence charge distributions shown in figures 2(*c*), 3(*c*) and 4(*c*) are calculated from the difference between the atomic valence Mulliken population (see, for example, Catlow and Stoneham (1983)) and the core charge.

3.1. Neutral chains

Our calculations on the neutral chains of all lengths confirm the expected picture of an almost uniform dimerization along the central conjugated part of the molecule. As the chains are shortened, we find that the calculated energy gap between the highest occupied and lowest unoccupied one-electron levels ($\pi - \pi^*$ gap) and the self-consistent energy difference between the lowest singlet and triplet states (see table 1) both increase because of the confinement of the carriers. Although, as we have said, care must be taken in comparing these energy differences with excitation energies, this behaviour is similar to the experimentally observed blue shift of the band-edge absorption in mini-carotenes as the chains are shortened (Andersson *et al* 1992).

Table 1. Singlet–triplet excitation energies in electronvolts as a function of chain length. The second column gives the excitation energy with the chain held rigid (see section 3.1), while the third column gives the formation energy for an exciton defect (see section 3.4). In both cases the energy change is calculated as the difference between two self-consistent total energies.

Molecule	Rigid chain	Exciton
Mini-3	4.58	3.18
Mini-5	3.91	2.29
Mini-7	3.61	1.81
Mini-9	3.47	1.52
Mini-11	3.20	1.30

3.2. Doubly charged chains

We performed full geometry optimizations on each of the five molecules with charge +2 and −2 in the singlet state. We shall discuss the results for the positively charged molecules first.

3.2.1. Dimerization. Figure 2(*a*) shows the dimerization pattern in two of the extreme chains of the group: mini-11 and mini-5. It suffices to analyse only these two since the behaviour of the other three chains follows a similar pattern. We see that the addition of the two charges to the chain causes a region of negative dimerization near the chain centre. In each case, the sign of the dimerization is chosen in such a way that positive dimerization is favoured at the ends of the conjugated segment; this is because the position of the double bond in the end rings is effectively fixed by the distribution of the hydrogen atoms. We see that positive terminal dimerization is indeed attained in the longest chain, leading to two changes of sign in the dimerization over the length of the chain. In the mini-5 chain, however, there is insufficient space for the dimerization to return to a positive value before the end of the chain is reached; in other words, the requirement for regions of rapidly varying dimerization to accommodate the additional carriers in solitonic defects (see below) is sufficient to outweigh the tendency to positive dimerization at the chain ends.

We interpret these dimerization patterns in terms of two charged solitons that repel each other to the ends of the conjugated chain. It is worth noting that, in a relatively short-chain molecule such as those studied here, the distinction between a pair of charged solitons, free to separate to a large distance, and a bipolaronic defect in which the two solitons are bound together is to some extent arbitrary. Our assignment to a pair of charged solitons in this case rests first on the observation that the two bond-alternation defects (points where the dimerization crosses zero) repel each other to near the ends of the chain, and second on the fact that β-carotene and its derivatives have a degenerate ground state (Heeger *et al* 1988); there is therefore no energy penalty associated with the reversal of dimerization and we have no theoretical grounds to expect a binding force between the solitons. Our assignment confirms that the picture arising from previous work on β-carotene itself (Ehrenfreund *et al* 1992a, b) applies to the whole family of mini-carotenes, but is modified by strong confinement of the solitons in the shorter-chain materials.

We find that the one-electron energy gap between the highest occupied and lowest empty state increases as the chain length is shortened. This suggests that there may be a blue shift in the optical absorption spectrum of doped mini-carotenes as the chain length is shortened, although we note that the greater confinement may also tend to increase the correlation energy of the photoexcited electron–hole pair and produce a competing red shift. Because of the well established difficulty in describing excited states in CNDO (see section 2) we do not attempt to predict optical absorption spectra in this paper.

3.2.2. Charge distribution. Figure 2(*b*) and (*c*) shows how the charge is distributed along the chains in mini-11 and mini-5 respectively. The alternating sign of successive atoms along the chain is characteristic of defects in conducting polymers (see, for example, Heeger *et al* (1988)). In both cases the charge is concentrated in two lobes located near the ends of the backbone and close to the terminal rings. We attribute these charge lobes to the presence of the two charged solitons near the ends of the chain (see section 3.2.1).

3.2.3. Charge-conjugation symmetry. For the negative doubly charged molecules the lattice distortion corresponds to the formation of a spinless pair of negatively charged solitons. These results are essentially identical to the results discussed above for the positive charges and are in agreement with experimental results obtained from doped α,ω-diphenyltetradecaheptaene, a closely related material in which the conjugated chain segment is terminated by completely conjugated benzene rings (Lögdlund *et al* 1993).

Owing to the inclusion of effects such as one-electron self-consistency and additional hopping terms in our approach, we do not find the simple symmetry of one-electron energy

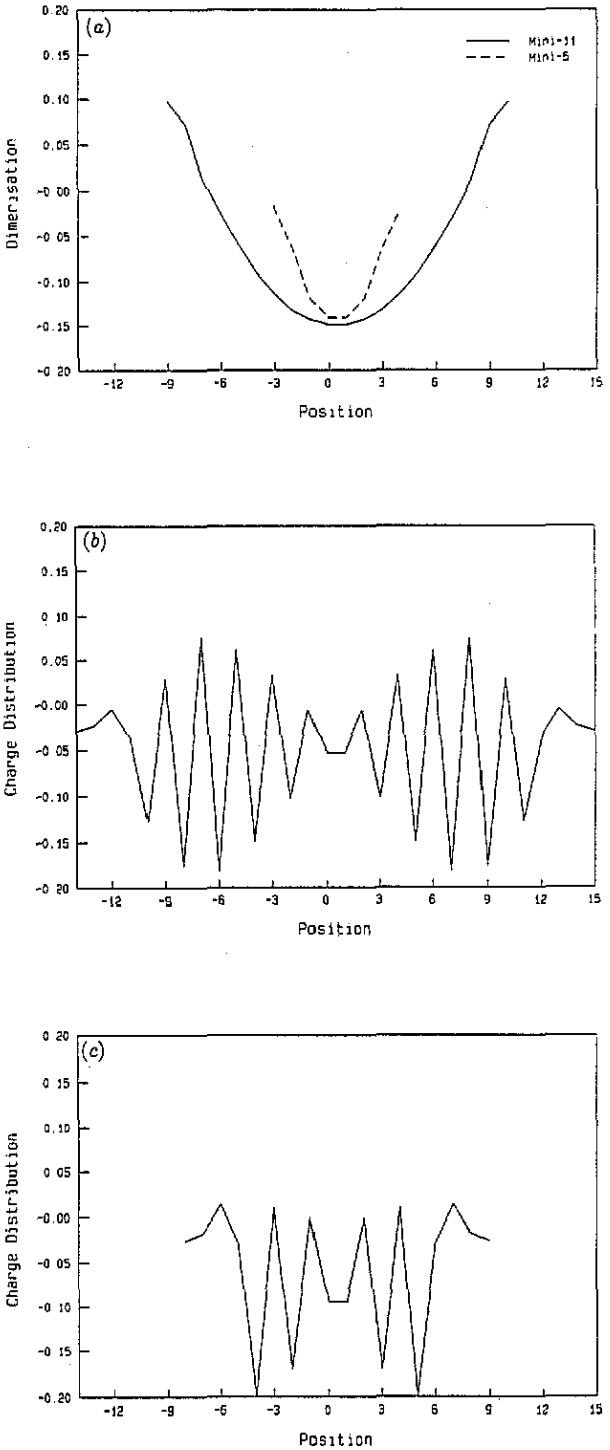

Figure 2. Results for chains carrying two positive charges: (*a*) dimerization parameter as a function of position along the conjugated backbone for mini-11 and mini-5; (*b*) charge distribution as a function of position along the chain for mini-11; (*c*) charge distribution as a function of position along the chain for mini-5.

levels about mid-gap that arises from CCS in the SSH model. We find, instead, a generalized form of CCS, which we illustrate in table 2. This table shows the one-electron HF eigenvalues corresponding to the valence and conduction band edges as well as those for the gap states for both the positively and negatively doubly charged mini-11 chain. We only include data from this chain length since the behaviour is similar for the shorter ones. We observe that the intervals between the eigenvalues of the negatively charged chain read from bottom to top are the same as the intervals between the eigenvalues of the positively charged chain read from top to bottom. For example, the intervals between the eigenvalues of the occupied states 76 and 77 in the chain with charge +2 is equal to the interval between the eigenvalues of the empty states 80 and 81 in the chain with charge −2, and so on. In other words, exchanging both the sign of the charge on the chain *and* the rôles of the conduction and valence bands (i.e. exchanging the occupied and unoccupied one-electron states) leaves the one-electron spectrum invariant. The only exception to this rule is the interval between the eigenvalues of the highest occupied and lowest unoccupied states in each case.

Table 2. Valence-band projections and eigenvalues for the doubly charged states. Eigenstates are numbered in order of increasing energy; the Fermi level for a neutral chain lies between the states numbered 78 and 79. The results for the occupied states are shown in bold roman type while the results for the unoccupied states are shown in italic type.

	Valence-band projections		Eigenvalues	
Eigenvector	Charge +2	Charge −2	Charge +2	Charge −2
76	**0.904**	**0.937**	**−0.586**	**−0.234**
77	**0.692**	**0.812**	**−0.542**	**−0.176**
78	*0.904*	**0.699**	*−0.276*	**−0.085**
79	*0.311*	**0.091**	*−0.242*	**−0.048**
80	*0.206*	*0.309*	*−0.155*	*−0.226*
81	*0.071*	*0.098*	*−0.103*	*−0.268*

It is also interesting to investigate how much of each individual state derives from the conduction band of the neutral (defect-free) chain and how much from the valence band. We can quantify this by defining a projection operator onto the valence-band wave functions of a neutral chain

$$\hat{P}_v^0 = \sum_{i \in v} |\psi_i^0\rangle\langle\psi_i^0| \tag{3a}$$

and studying its expectation value

$$S_j = \langle\psi_j|\hat{P}_v^0|\psi_j\rangle = \sum_{i \in v} \langle\psi_j|\psi_i^0\rangle\langle\psi_i^0|\psi_j\rangle \tag{3b}$$

in the filled and empty states of the charged chain. These projections, shown for the states near the Fermi energy in table 2, are a measure of the amount of each state that is derived from the valence band of the neutral chain. We see that the values of S_j for the chain of charge −2 can be obtained from those of charge +2 by inverting the table through the neutral-chain Fermi level (i.e., interchanging states 78 and 79, 77 and 80, 76 and 81 and so on) while at the same time replacing S_j by $(1 - S_j)$ (i.e., exchanging projection onto the neutral-chain conduction and valence bands). The generalized CCS exhibited by the eigenvalues is therefore also found for the projections.

It is interesting to note that the positive experimental tests of CCS (see, for example, Swanson *et al* (1992) for ODMR results on the polymer PPV) usually relate properties of positively and negatively charged defects. They therefore test precisely the generalized CCS found in the present calculations, and not the stronger symmetry of one-electron levels about mid-gap that is predicted by the SSH model.

3.3. Polarons

We have also applied our method to the singly charged (spin-$\frac{1}{2}$) molecules mini-11 to mini-3. Once again the calculations were carried out for both positive and negative charges. The molecules now have non-zero spin; we choose this spin so there are always more spin-up (α) electrons than spin-down (β) electrons, but this choice has no physical significance. As with the doubly charged chains we only include the dimerization pattern and charge distribution figures for the longest (mini-11) and second shortest (mini-5) chains in the series since the others follow the trends presented by these two.

3.3.1. Dimerization. There is a marked relaxation of the structure in the middle of the molecules where the bond alternation is almost completely suppressed, although the dimerization does not actually change sign in this case. This relaxation extends over 15–17 carbons for mini-11 and over 6–8 carbons in mini-5 (see figure 3(a)). The lattice distortion corresponds to that of a polaron, and reproduces the results obtained with the same method for t-PA (Wallace 1989). In all cases the polaron lies entirely on the chain and does not invade the end rings; as with the doubly charged molecules we see that confinement results in a compression of the defect when going from the long to the short chains. These confinement effects increase the one-electrom energy differences between filled and empty states as the chain shortens, as in the doubly charged chains.

3.3.2. Charge distribution. Figure 3(b) and (c) shows how the charge associated with a positive polaron is stored along the chains of mini-11 and mini-5 respectively. As in the case of the doubly charged molecules the charge is concentrated in two lobes, which are positioned at the ends of the chains, close to the end groups. The polaron defect can be thought of as a bound state of a charged and a neutral soliton, each forming one side of the dip in the dimerization curve. The wave function of the unpaired electron is then a bonding or antibonding combination of the mid-gap states associated with the two solitons. This explains why the largest amplitude for the wave function is at the edges of the defect, where the dimerization is changing most rapidly.

The charge here is more localized than in the doubly charged chains; one would expect this since the Coulomb repulsion between the two additional electrons present in the doubly charged molecules is absent here.

3.3.3. Charge-conjugation symmetry. The results for the negative singly charged molecules are similar to those obtained with the positive singly charged molecules: the lattice distortion for a negative polaron has the same characteristics as the positive one. In table 3 we present the eigenvalues and valence-band projections (calculated from equations (3)) for the valence and conduction band edges as well as for the gap states in the α and β spin for both positive and negative polarons. Once more the results exhibit a modified CCS the spectrum of eigenvalues corresponding to the negative polaron's α spin read from bottom to top has the same behaviour as the spectrum corresponding to the positive polaron's β spin read from top to bottom. Similarly the negative polaron's β-spin spectrum read from top to bottom coincides with the positive polaron's α-spin spectrum read from bottom to

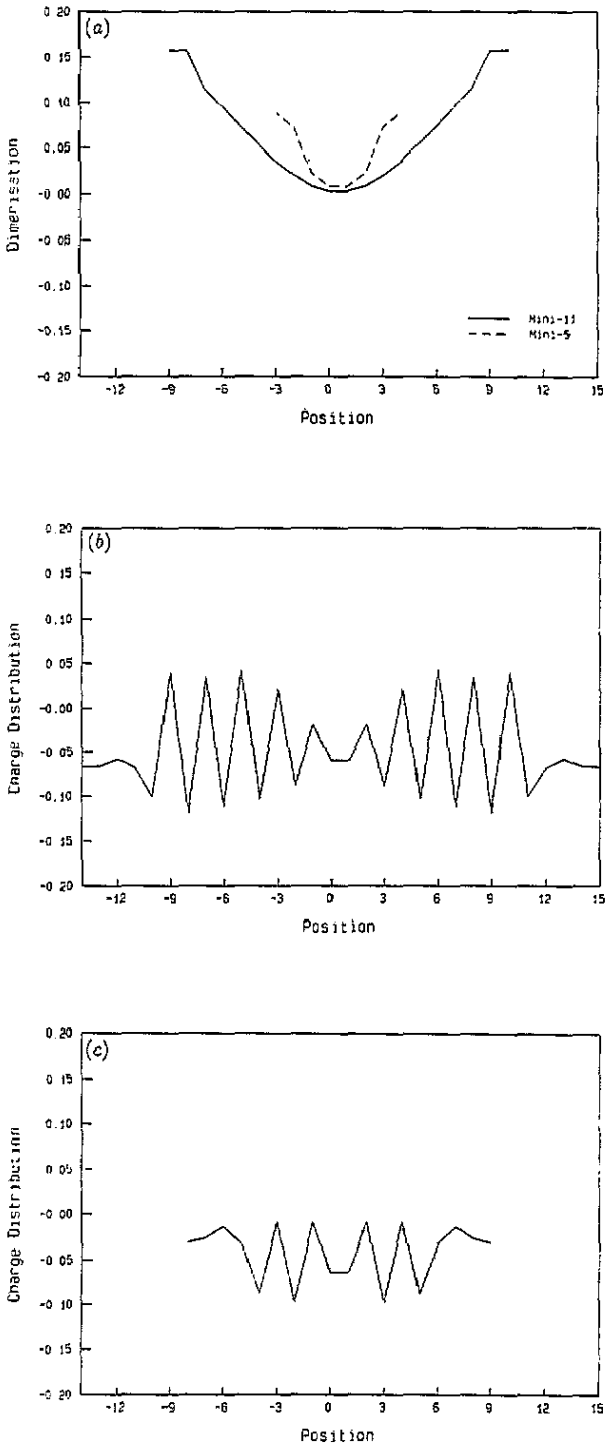

Figure 3. Results for chains carrying a single positive charge: (*a*) dimerization parameter as a function of position along the conjugated backbone for mini-11 and mini-5; (*b*) charge distribution as a function of position along the chain for mini-11; (*c*) charge distribution as a function of position along the chain for mini-5.

top. As was the case for the doubly charged chains, the only significant exception to this rule comes in the HOMO–LUMO excitation energies, which are somewhat different for the two charge states.

Table 3. Valence-band projections and eigenvalues for states of the singly charged chains. The eigenstates are numbered in order of increasing energy; the Fermi level for a neutral chain lies between the states numbered 78 and 79. Results for occupied states are shown in bold roman type and those for unoccupied states in italic type.

	Valence-band projections				Eigenvalues			
	Charge +1		Charge −1		Charge +1		Charge −1	
Eigenvector	α	β	α	β	α	β	α	β
77	**0.995**	**0.844**	**0.937**	**0.993**	**−0.457**	**−0.489**	**−0.227**	**−0.258**
78	**0.995**	*0.998*	**0.813**	**0.997**	**−0.410**	*−0.384*	**−0.211**	**−0.167**
79	*0.003*	*0.183*	**0.004**	*0.005*	*−0.160*	*−0.308*	**−0.120**	*0.088*
80	*0.008*	*0.065*	*0.168*	*0.004*	*−0.074*	*−0.286*	*0.131*	*0.136*

3.3.4. Relative stability of charge states. We define E_n to be the total energy of charge n, and calculate the energy difference between two infinitely separated singly charged chains and a neutral chain plus a doubly charged chain:

$$2E_{+1} - (E_0 + E_{+2}) = -0.066\,\text{au}(= -1.7960\,\text{eV})$$
$$2E_{-1} - (E_0 + E_{-2}) = -0.072\,\text{au}(= -1.9592\,\text{eV}).$$

Our method therefore predicts the singly charged chains to be more stable than the doubly charged ones in both positive and negative cases. This result, however, disagrees with the experiments reported by Ehrenfreund *et al* (1992a, b), which suggested that the most stable form for charge storage at high doping levels is a spinless species.

We suggest two possible explanations for this discrepancy. First, the above estimate compares the energy of two isolated singly charged chains with that of a single doubly charged chain. In the real situation, though, chains interact. We have estimated the Coulomb interaction energy of two singly charged chains separated by the extent of a molecule as a more representative case. This energy is 0.0625 au, which is comparable to the energy differences calculated above. In other words, in real systems the singly charged chains repel each other and may not therefore be significantly more stable than the doubly charged ones.

A second possible explanation for this discrepancy between theory and experiment is that our calculations do not include correlation effects. Such effects might be expected to lower the energy of doubly charged chains relative to the singly charged ones, since they enable two charges on the same chain to avoid each other more efficiently while still enjoying the energetic benefits of a shared lattice distortion.

3.4. Excitons

Having examined the charged defects that can be produced by doping of the β-carotene homologues, we now turn to the neutral defects (excitons) formed after an electron and a hole have been produced by optical excitation. This defect was modelled as the lowest lying triplet state in order to allow a self-consistent calculation to be performed without

the system collapsing into its ground state. Because CNDO does not consider interatomic exchange terms, we expect that the singlet and triplet states will in any case have very similar properties.

The calculated energy of formation of this defect in the full-length β-carotene chain (mini-11) is 0.0478 au (1.30 eV). This compares with the energy to produce an electron–hole pair at frozen geometry of 0.1249 au (3.40 eV); the difference is due to the lattice relaxation. Notice also that both these energies are much less than the excitation energy that one would estimate from simple one-electron energy differences (Koopman's theorem) at a fixed geometry. The corresponding numbers for other chain lengths are shown in table 1.

3.4.1. Dimerization. Figure 4(a) shows the distortion pattern of an exciton in β-carotene and its lower homologue mini-5. As in the case of t-PA (Wallace 1989) the bond-length alternation in the centre of the chain is reduced. The general shape of the dimerization curve is very similar to that obtained for t-PA (Wallace 1989). The spread of the defect along the β-carotene chain is over 17 bond lengths, while the extent in a long chain would be around 20 bond lengths. The dimerization enhancement associated with the ends of a polymer chain is present, as it was in the ground state. This behaviour corroborates the results of Coter *et al* (1991) in that it seems to indicate that the end rings do not play a significant role in the behaviour of this molecule.

If one compares figures 2(a) and 4(a) one can see that although the maximum distortion is similar in each case, the exciton's distortion is much sharper than that observed for the doubly charged molecules. We believe that this is because the Coulomb repulsion between the charged solitons in the charged chains is absent in chains containing an exciton.

3.4.2. Spin distribution. Since this defect is neutral, it is more helpful to analyse the spin than the charge distribution along the chains. figures 4(b) and 4(c) show the valence spin distribution for mini-11 and mini-5 respectively; in both cases the spin is localized in two lobes near to the end rings. This situation is similar to that encountered for the charge distribution in both the singly and doubly charged chains.

4. Conclusions

Our self-consistent semi-empirical calculations carried out on the oligomers of the β-carotene family yield configurations for charged and neutral defects similar to those that might be expected if the molecule is viewed as a degenerate conjugated polymer. For doubly charged chains we predict the formation of a pair of charged solitons while in the case of the singly charged chains we find formation of polaron-like defects. The excited state of the neutral chain forms excitons very similar to those found in t-PA. In all cases we have analysed the defects as a function of chain length and find that chain shortening produces confinement effects. These confinement effects manifest themselves through the calculated charge distributions (spin distribution in the case of the exciton), which are compressed as the chains shorten.

Although our results suggest that the (positive and negative) doubly charged chains are both unstable relative to a pair of infinitely separated singly charged chains, we propose that, because of the finite concentration of dopants, singly charged chains are destabilized by their mutual Coulomb interaction and are not significantly more stable than the doubly charged ones. This may have consequences for the transport properties of doped mini-carotenes.

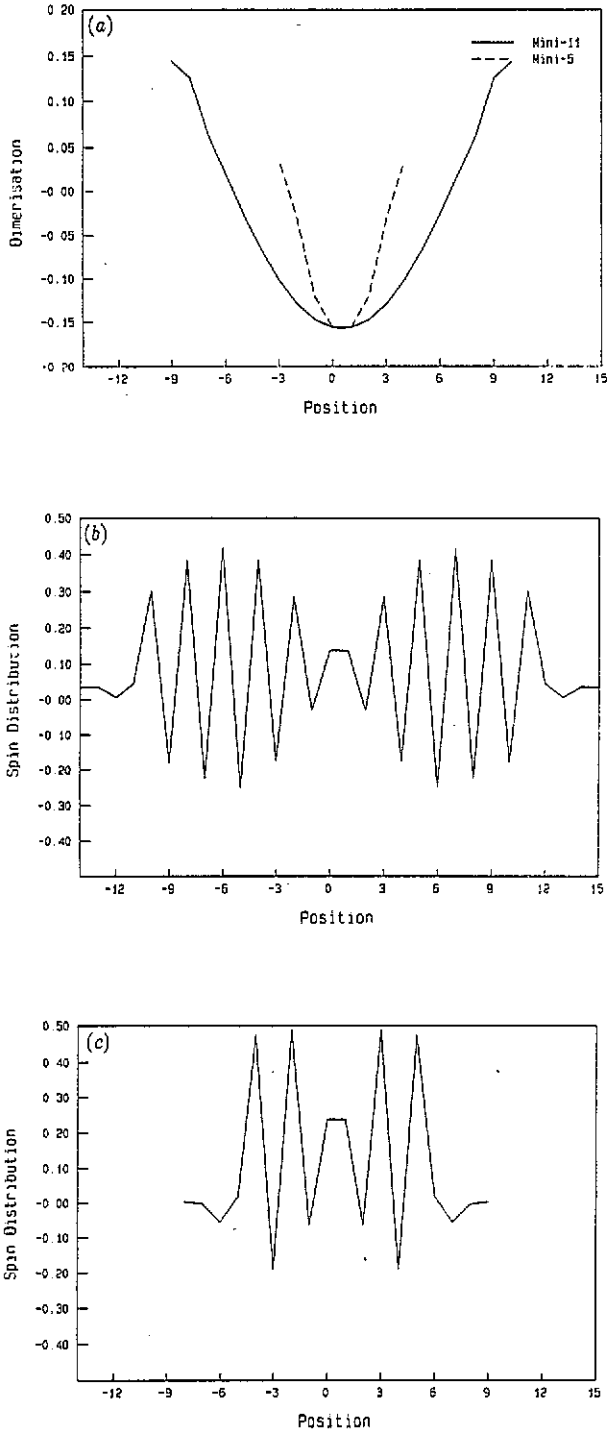

Figure 4. Results for neutral chains in the presence of a triplet exciton: (*a*) dimerization parameter as a function of position along the conjugated backbone for mini-11 and mini-5; (*b*) spin distribution as a function of position along the chain for mini-11; (*c*) spin distribution as a function of position along the chain for mini-5.

A particularly interesting feature of our results is the appearance of a generalized form of CCS in the charged molecules that relates the properties of positively and negatively charged chains. In contrast with the CCS exhibited by the SSH model, the one-electron levels are no longer symmetric about mid-gap; instead, the eigenvalue spectrum and the composition of the one-electron states are invariant under change in the sign of the defect charge and exchange of valence and conduction bands. This generalized CCS appears to be consistent with the available experimental data.

Acknowledgments

We thank the Commission of the European Communities for support under grant CEC C11-CT92-0102. RMV is grateful to DGAPA and IIM, Universidad Nacional Autónoma de México, for support. AJF thanks St John's College, Oxford, for the award of a Junior Research Fellowship.

References

Andersson P O, Gillbro T, Asato A E and Liu R S H 1992 *J. Lumin.* **51** 11
Brédas J L and Heeger A J 1989 *Chem. Phys. Lett.* **154** 56
Brédas J L, Silbey R, Boudreaux D S and Chance R R 1983 *J. Am. Chem. Soc.* **105** 6555
Brédas J L and Toussaint J M 1990 *J. Chem. Phys.* **92** 2624
Burroughes J H, Bradley D D C, Brown A R, Marks R N, Mackay K, Friend R H, Burns P L and Holmes A B 1990 *Nature* **347** 539
Car R and Parrinello M 1985 *Phys. Rev. Lett.* **55** 2471
Catlow C R A and Stoneham A M 1983 *J. Phys. C: Solid State Phys.* **16** 4321
Chiang C K, Fincher C R, Park Y W, Heeger A J, Shirakawa H, Louis E J, Gau S and MacDiarmid A G 1977 *Phys. Rev. Lett.* **39** 1098
Coter F, Ehrenfreund E and Horovitz B 1991 *Synth. Met.* **41–43** 1259
Ehrenfreund E and Coter F 1991 private communication
Ehrenfreund E, Hagler T W, Moses D, Wudl F and Heeger A J 1992a *Synth. Met.* **49–50** 77
Ehrenfreund E, Moses D, Heeger A J, Cornil J and Brédas J L 1992b *Chem. Phys. Lett.* **196** 84
Fisher A J, Hayes W and Pratt F L 1991 *J. Phys.: Condens. Matter* **3** L9823
Heeger A J, Kivelson S, Schrieffer J R and Su W-P 1988 *Rev. Mod. Phys.* **60** 781
Kohler B E 1991 *Conjugated Polymers* ed J L Brédas and R Silbey (Dordrecht: Kluwer Academic)
Lögdlund M, Dannetun P, Stafström S, Salaneck W R, Ramsey M G, Spangler C W, Fredriksson C and Brédas J L 1993 *Phys. Rev. Lett.* **70** 970
Rosenberg B 1959 *J. Chem. Phys.* **31** 238
Roth S and Bleier H 1987 *Adv. Phys.* **36** 385
Shuai Z and Brédas J L 1992 *J. Chem. Phys.* **97** 5970
Swanson L S, Shinar J, Lane P A, Hess B C and Wudl F 1992 *Synth. Met.* **49–50** 481
Su W-P, Schrieffer J R and Heeger A J 1979 *Phys. Rev. Lett.* **42** 1698
—— 1980 *Phys. Rev.* B **22** 2099
Wallace D S 1989 *DPhil Thesis* University of Oxford; *AERE Report* TP.1331
Wallace D S, Stoneham A M, Hayes W, Fisher A J and Harker A H 1991a *J. Phys.: Condens. Matter* **3** 3879
Wallace D S, Stoneham A M, Hayes W, Fisher A J and Testa A 1991b *J. Phys.: Condens. Matter* **3** 3905